

Figure 1. Observed rotation as a function of irradiation time at 25° for a solution of 0.00050 M Cr(phen)₃Cl₃ obtained by ion exchange separation from a solution 0.00073 M in complex containing 3% potassium antimony D-tartrate. The latter solution was the one irradiated. (The dilution was necessary to achieve complete recovery of the complex from the resin.) Note that the half-time for photoracemization of a comparable resolved sample was 27 min.

half-time of 27 min at 25° under unpolarized illumination with the 350-nm lamps of a Rayonnet photoreactor. Light intensity in the reactor was gauged by ferrioxalate actinometry.⁶ The quantum yield for isomerization is approximately 0.016. Thermal racemization is entirely negligible ($t^{1/2} \approx 17$ days at 25°).

Figure 1 shows rotations at 546 nm achieved by irradiating comparable solutions of *racemic* Cr(phen)₃³⁺ in the presence of antimony D-tartrate. These are reported as rotations of the metal complex after separation of the total sample from the dextrorotatory anion on a Dowex I-X4 anion-exchange column (chloride form). The levorotatory isomer predominates. (In the absence of irradiation, the work-up yields inactive solutions.) Figure 1 indicates that the system approaches a steady-state rotation after 88 min of irradiation, which corresponds to three racemization half-lives for resolved Cr(phen)₃Cl₃. The steady-state rotation corresponds to a 1.7% resolution. An essentially identical degree of photoresolution was achieved using an initial complex concentration of 0.0004 M. This is consistent with the absence of a specific chloride counterion effect on photoisomerization.⁴ A slightly higher percentage resolution was obtained in 6% antimony D-tartrate (2.4%).

Table I shows the steady-state specific rotations compared to a resolved sample at the several wavelengths available on the Perkin-Elmer 141 polarimeter used in this study. They are consistent with the attribution of

Table I. Comparison of Steady-State Specific Rotation with (+)₅₈₉-Cr(phen)₃Cl₃

λ , nm	436	546	578	589
$[\alpha]_{\text{steady state}}$	-53.1	-28.4	-24.0	-21.9
$[\alpha]_{\text{((+) - Cr(phen)}_3\text{Cl}_3\text{)}}$	+3460	+1716	+1402	+1320

steady-state rotation to Cr(phen)₃³⁺. Further, the partially photoresolved samples undergo photoracemization in times similar to photoracemization of the conventionally resolved complex.

Irradiation of solutions for periods considerably longer than those shown in Figure 1 results in photosubstitution of resolving agent for a coordinated phenan-

(6) C. G. Hatchard and C. S. Parker, *Proc. Roy. Soc., Ser. A*, **235**, 518 (1956).

tholine. Under these conditions, a highly levorotatory orange solution is obtained after separation on the anion resin. The relative rotations at the Perkin-Elmer wavelengths available are markedly different from those shown in Table I. In addition, this species was not observed to photoracemize.

Noel A. P. Kane-Maguire, Barbara Dunlop, Cooper H. Langford*

Department of Chemistry, Carleton University
Ottawa, Canada K1S 5B6

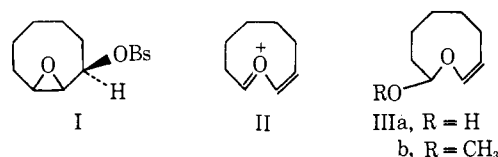
Received July 19, 1971

Evidence for a Change in Rate-Determining Step in the Acid-Catalyzed Hydrolysis of a Vinyl Ether

Sir:

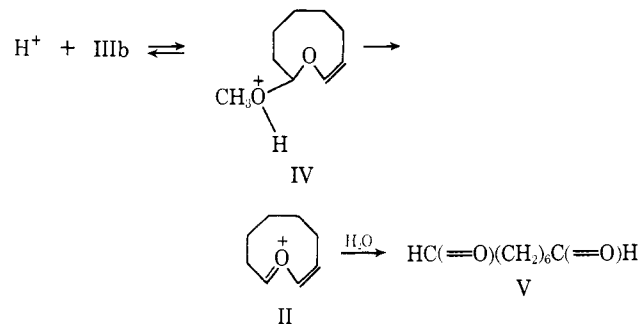
During the past few years there has been intense interest in the detailed mechanisms of the acid-catalyzed hydrolyses of acetals¹ and vinyl ethers.² Part of this interest stemmed from a desire to understand catalytic processes in detail,^{1a,2a-g} while renewed interest in the mechanism of acetal hydrolysis has been stimulated by the resemblance of their hydrolytic processes to the action of certain glycosidic enzymes.^{1a,b}

In this communication we wish to report the synthesis of 9-methoxyoxacyclonon-2-ene³ (IIIb), and the kinetic investigation⁴ of its hydrolysis in wholly aqueous



buffered solutions. In acid solutions, this material can potentially hydrolyze by two main mechanisms, *i.e.*, initial protonation on endocyclic or exocyclic oxygen atoms of IIIb followed by rate-determining cleavage to a stabilized oxonium ion¹ (A-1 mechanism, Scheme I), or

Scheme I. A-1 Hydrolysis Mechanism



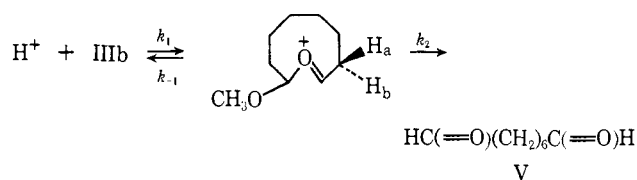
(1) (a) E. H. Cordes, *Progr. Phys. Org. Chem.*, **4**, 1 (1967); (b) E. Anderson and T. H. Fife, *J. Amer. Chem. Soc.*, **93**, 1701 (1971); (c) H. G. Bull, K. Koeler, T. C. Pletcher, J. J. Ortiz, and E. H. Cordes, *ibid.*, **93**, 3002 (1971), and references contained therein.

(2) (a) A. J. Kresge, H. L. Chen, Y. Chiang, E. Murrill, M. A. Payne, and D. S. Sagatys, *ibid.*, **93**, 413 (1971); (b) A. J. Kresge and Y. Chiang, *J. Chem. Soc. B*, **53**, 58 (1967); (c) M. M. Kreevoy and R. Eliason, *J. Phys. Chem.*, **72**, 1313 (1968); (d) V. Gold and D. C. A. Waterman, *J. Chem. Soc. B*, 839 849 (1969); (e) T. H. Fife, *J. Amer. Chem. Soc.*, **87**, 1084 (1965); (f) T. Okuyama, T. Fueno, H. Nakatsujii, and J. Furakawa, *ibid.*, **89**, 5826 (1967); (g) G. Lienhard and T. C. Wang, *ibid.*, **91**, 1146 (1969); (h) P. Salomaa, A. Kankaanperä, and M. Lajunen, *Acta Chem. Scand.*, **20**, 1790 (1966).

(3) The Hantzsch-Widman method for naming IIIb is 2-methoxy-2,3,4,5,6,7-hexahydrooxonine, IUPAC 1957 Rules for Nomenclature of Organic Chemistry, *J. Amer. Chem. Soc.*, **82**, 5445 (1960), Section B-1.

(4) The kinetics were followed spectrophotometrically with a Gilford Model 2400 spectrophotometer by monitoring the disappearance of starting material at 210–225 nm.

Scheme II. Vinyl Ether Hydrolysis Mechanism



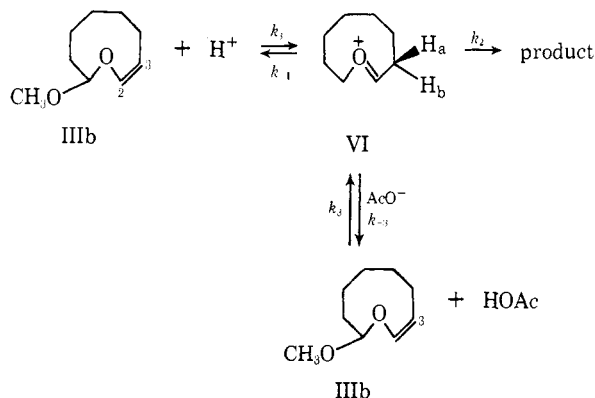
initial protonation on carbon (vinyl ether hydrolysis mechanism,² Scheme II).

Our kinetic results, discussed in detail below, have shown that IIIb hydrolyzes predominately *via* the mechanism illustrated in Scheme II, and furthermore provide evidence that there is a change in rate-determining step with changing buffer concentration.

One of us recently reported⁵ that the solvolysis of *syn*-9-oxabicyclo[6.1.0]non-2-yl *p*-bromobenzenesulfonate (I) in aqueous acetone yielded 51% suberaldehyde (V), and postulated an intermediate oxonium ion, II. Collapse of this ion with water yields the hemiacetal IIIa, and rearrangement of IIIa would provide the observed dialdehyde. We have now carried out the solvolysis of I in anhydrous, buffered (triethylamine) methanol and obtained a 52% yield⁶ of the corresponding acetal IIIb: *uv* (cyclohexane) 215 nm (ϵ 494); *ir* (CCl₄) 3040, 1660 cm⁻¹; *nmr* (CCl₄) δ 6.05 (d, 1, J = 6 Hz, OCH=C), 4.85 (quartet, 1, J = 6 Hz, OC=CH) 4.49 (t, 1, CHOCH₃), 3.35 (s, 3, OCH₃), 2.1 (m, 2, C=CCH₂), 1.6 ppm (m, 8); M^+ (mass spectrum) 156. The value of 6 Hz for the olefinic coupling constant $J_{2,3}$ indicates a *cis* stereochemistry for the double bond in IIIb.

In dilute aqueous hydrochloric acid solution, IIIb is converted cleanly to suberaldehyde, $k_H = 8.1 \pm 0.2 M^{-1} \text{sec}^{-1}$, at 25.1°. In DCl-D₂O solution, $k_D = 1.94 \pm 0.05 M^{-1} \text{sec}^{-1}$. Thus the solvent isotope effect (k_{H_2O}/k_{D_2O}) for the hydronium-ion-catalyzed reaction is 4.2 ± 0.2 . This large, maximum⁷ solvent isotope effect is evidence against a mechanism involving a fast pre-equilibrium protonation of oxygen (Scheme I), and clearly establishes that the proton-transfer step (k_1) of the hydronium-ion-catalyzed reaction (Scheme II) is rate determining.^{2a-e,g,h} However, unlike most vinyl ethers,^{2a-e,g,h} which show a linear increase of k_{obsd} with increasing buffer acid concentration at constant

Scheme III



(5) D. L. Whalen, *J. Amer. Chem. Soc.*, **92**, 7619 (1970).

(6) The product was separated by preparative glpc on a 3/8-in., 10% SE-30 column.

(7) A. J. Kresge, D. S. Sagatys, and H. L. Chen, *J. Amer. Chem. Soc.*, **90**, 4174 (1968).

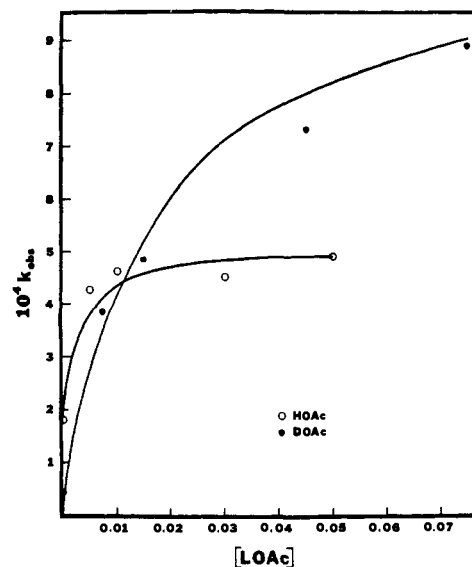


Figure 1. Plot of k_{obsd} vs. HOAc (DOAc) at pH (pD) = 4.65 ± 0.01 and 25.1° ; ionic strength = 0.1 (NaCl).

pH, the relationship between k_{obsd} and buffer acid concentration for IIIb is decidedly nonlinear (see Figure 1).

The above results can be very well accommodated by Scheme III. Steady-state approximation for VI provides the expression for k_{obsd} given by

$$k_{\text{obsd}} = \frac{(k_1[\text{H}^+] + k_3[\text{HOAc}])k_2}{k_{-1} + k_{-3}[\text{AcO}^-] + k_2} \quad (1)$$

The magnitude of the solvent isotope effect in the absence of a buffer strongly suggests that $k_{-1} \ll k_2$. Thus

$$k_{\text{obsd}} = \frac{k_1[\text{H}^+] + k_3[\text{HOAc}]}{1 + (k_{-3}/k_2)[\text{AcO}^-]} \quad (2)$$

The solid curves in Figure 1 reproduce the experimental points with an average deviation of $\pm 6\%$ and were calculated with the following constants:⁸ $k_1^H = 8.2 \pm 0.2 M^{-1} \text{sec}^{-1}$, $k_3^H = 0.196 \pm 0.020 M^{-1}$, $(k_{-3}/k_2)^H = 387 \pm 47 M^{-1}$; $k_1^D = 1.94 \pm 0.05 M^{-1} \text{sec}^{-1}$, $k_3^D = 0.062 \pm 0.004 M^{-1} \text{sec}^{-1}$, $(k_{-3}/k_2)^D = 186 \pm 18 M^{-1}$. The large value of the ratio k_{-3}/k_2 demands that at high concentrations of HOAc-AcO⁻, VI is formed rapidly and reversibly.⁹ The rate-determining step therefore involves some subsequent reaction.¹⁰ The limiting solvent isotope effect under these conditions, calculated from the above constants, is 0.46 ± 0.10 . This *inverse* isotope effect is expected for reactions involving a pre-equilibrium protonation.¹¹

(8) Equation 2 may be rearranged to yield

$$\frac{k_{\text{obsd}} - k_1[\text{H}^+]}{[\text{HOAc}]} = -\left(\frac{k_{-3}}{k_2}\right)\left(\frac{k_{\text{obsd}}}{R}\right) + k_3$$

where R = buffer ratio, $[\text{HOAc}]/[\text{AcO}^-]$. The constants mentioned in the text were obtained by a least-squares analysis of plots of $(k_{\text{obsd}} - k_1[\text{H}^+])/[\text{HOAc}]$ vs. k_{obsd}/R . There were 21 points used to obtain the HOAc constants and 15 to obtain the DOAc constants.

(9) The *nmr* spectrum of unreacted IIIb, isolated after 1.7 half-lives in 0.05 *M* DOAc-0.017 *M* NaOAc solution, did not indicate exchange ($\geq 10\%$) of the vinylic hydrogen H_a. This result indicates that H_a and H_b in VI undergo exchange at significantly different rates.

(10) At this time we have no firm evidence concerning which step is rate determining, although collapse of VI with water to yield a hemiacetal is an attractive possibility.

(11) F. A. Long, *Ann. N. Y. Acad. Sci.*, **84**, 596 (1960); R. L. Schowen, *Progr. Phys. Org. Chem.*, in press.

The hydrolysis of IIIb therefore provides the first example of a change in rate-determining step in the hydrolysis of a vinyl ether.¹²

Acknowledgment. We wish to thank Dr. R. M. Pollack and Dr. A. S. Hyman for several informative discussions. Thanks are also due Dr. C. C. Fenselau for the mass spectrometric analysis of IIIb. This work was supported in part by the National Science Foundation (V.P.V.) and the Research Corporation (D. L. W.).

(12) It should be pointed out that Kankaanperä has recently investigated the hydrolytic behavior of a related substrate, 2-ethoxy-2,3-dihydropyran: A. Kankaanperä, *Acta Chem. Scand.*, **23**, 1465 (1969). On the basis of a slightly inverse solvent isotope effect, solvent isotope effects in H₂O-D₂O mixtures, and activation parameters, he concluded that this substrate hydrolyzes by *concurrent* acetal and vinyl ether pathways (Schemes I and II). Unfortunately, no buffer experiments were reported, and a firm decision regarding the hydrolysis mechanism of this material must await further work now in progress in our laboratory.

J. D. Cooper, V. P. Vitullo,* D. L. Whalen*

Department of Chemistry
University of Maryland Baltimore County
Baltimore, Maryland 21228

Received July 22, 1971

Electron Spectroscopy of Platinum-Oxygen Surfaces and Application to Electrochemical Studies

Sir:

Several papers have recently appeared^{1,2} where the authors discuss the electron distribution for a variety of platinum compounds *via* observed shifts in core electron binding energies. ESCA is a powerful technique for studying the surface properties of metals and already shows promise as a tool in elucidating mechanisms of heterogeneous catalysis.¹ In this study we wish to report direct spectral observation of chemisorbed oxygen on a platinum surface and to report binding energies for oxides produced from chemical oxidation of the platinum substrate. In addition, these results will be applied to the investigation of an electrochemically perturbed platinum electrode in an attempt to more clearly elucidate the types of oxides which are observed. Although the spectral measurements cannot be performed in the electrochemical cell the unequivocal chemical identification of electrochemically formed surface compounds would aid tremendously in interpreting the corresponding current-potential behavior.

The large ionization cross section for the Pt 4f electrons as well as the natural conductivity of platinum yield very high counting rates with a minimum of experimental complexity. Sample pretreatment consists either of etching a 0.5-cm² platinum foil with hot aqua regia, followed by (a) reduction with hydrogen at 400° or (b) reduction with FeSO₄. All cleaned platinum samples for the 4f(5/2) and 4f(7/2) lines exhibit a distinct asymmetric shape slanted toward high binding energies and the peak area ratios deviate from the theoretical value of 1.33. Delgass¹ suggested that the low ratio for a pre-reduced platinum foil was due to platinum oxide on the surface. This effect has also been observed for platinum

(1) W. N. Delgass, T. R. Hughes, and C. S. Fadley, *Catal. Rev.*, **4**, 179 (1970).

(2) (a) C. D. Cook, K. Y. Wan, U. Gelius, K. Hamrin, G. Johansson, E. Olsson, H. Siegbahn, C. Nordling, and K. Siegbahn, *J. Amer. Chem. Soc.*, **93**, 1904 (1971); (b) D. T. Clark, D. B. Adams, and D. Briggs, *Chem. Commun.*, 601 (1971).

which has been vapor deposited within the sample chamber at 10⁻⁵ Torr.³ Pure PtO₂ has symmetric 4f bands with the proper peak area ratio of 1.33. Siegbahn⁴ and Clark^{2b} have reported symmetric Pt 4f bands in numerous platinum complexes. Pure gold, on which oxygen is not strongly adsorbed, has very symmetric 4f bands with a peak area ratio of 1.33 using our spectrometer. Thus, the platinum surfaces have two chemical environments for the Pt, and using unskewed gaussian shapes, we could resolve the spectra into two distinct sets each with the 1.33 ratio (see Figure 1a). Coupled with the presence of a strong and symmetrical O 1s peak (half-band width 1.5 eV) at 531.8 eV⁵ and the known tendency of oxygen to rapidly chemisorb on the clean platinum surface,⁶ the second species (see Table I for binding energies) is

Table I. Binding Energies in Electron Volts for Oxidized Platinum Surfaces^a

A	Nitric acid —treatment ^b —		Half-band widths 4f(7/2)	Rel peak areas, %
	4f(7/2)	4f(5/2)		
Pt	70.7	74.0	1.2	41
PtO _{ads}	71.8	75.1	1.9	39
PtO	73.4	76.6	1.3	14
PtO ₂	74.2	77.5	1.2	6

B	Electrochem treatment ^c		—Rel peak areas at—		
	4f(7/2)	4f(5/2)	+0.7 V ^d	+1.2 V	+2.2 V
Pt	70.7	74.0	56	39	34
PtO _{ads}	71.6	74.9	39	37	24
PtO	73.3	76.6	<5	24	22
PtO ₂	74.1	77.4	0	0	20

^a Spectra obtained on a Hewlett-Packard Model 5950A using monochromatic Al X-rays. Bands resolved on a Du Pont Model 310 curve resolver. ^b Refluxed for several hours in concentrated HNO₃. ^c 1 M HClO₄. ^d Oxidation potential held at indicated potential for 3 min; freshly reduced electrode is taken before each run.

undoubtedly due to chemisorbed oxygen. Note that for physically adsorbed oxygen, a doublet O 1s band would be expected due to the paramagnetic character of molecular oxygen.⁷ We have always observed the presence of a C 1s band on the platinum surface although

(3) J. Lester, Northwestern University, private communication.

(4) K. Siegbahn, C. Nordling, A. Fahlman, R. Nordberg, K. Hamrin, G. Hedman, G. Johansson, T. Bergmark, S. Karlsson, I. Lindgren, and B. Lindberg, "ESCA; Atomic, Molecular and Solid State Structure Studied by Means of Electron Spectroscopy," Almquist and Wiksells, Boktryckeri AB, Uppsala, 1967, p 25.

(5) All binding energies are reported with respect to graphite, C 1s, as 284.0 eV. The half-band widths for the 7/2 and 5/2 bands were assumed to be equal for the first deconvolution. Then the half-band widths were adjusted to obtain the best fit. In general the 7/2 band was about 0.1 eV narrower. In the complex spectra (as Figure 1c) the peak ratio was held at 1.33 to complete the deconvolution. The metallic platinum bands on the pure surface are fit by a lorentzian shape a bit better than by a gaussian shape; however, the nonmetallic platinum oxides have gaussian band shapes.

(6) D. O. Hayward and D. M. W. Trapnell, "Chemisorption," Butterworths, London, 1964.

(7) K. Siegbahn, C. Nordling, G. Johansson, J. Hedman, P. F. Heden, K. Hamrin, U. Gelius, T. Bergmark, L. O. Werme, R. Manne, and Y. Bear, "ESCA Applied to Free Molecules," North Holland, Amsterdam, 1969, p 56.